

# Structural and Electrical Properties of Sr - Substituted Perovskites Nano crystalline $\text{La}_{1-x}\text{Sr}_x\text{MnO}_3$

G.N.Chaudhari, A.B.Bodade, D.K.Burghate

Department of Chemistry, Shri Shivaji Science College, Amravati-444603

Department of Physics, Science College, Nagpur

**Abstract**— A series of polycrystalline  $\text{La}_{1-x}\text{Sr}_x\text{MnO}_3$  ( $x=0, 0.15, 0.3, 0.45$ ) compound have been synthesized by sol-gel method. X-ray diffraction analysis revealed the nano crystalline nature of  $\text{La}_{1-x}\text{Sr}_x\text{MnO}_3$ . The electrical properties for all the samples have been studied as a function of frequency in the range 42 Hz–50 MHz and temperature range 30-700.<sup>o</sup>c The appearance of peak in imaginary part of impedance (Z'') for each concentration and shifting of this peak with temperature towards higher frequency side indicated that the presence of electric relaxations.

**Key words:**- $\text{LaMnO}_3$  (LMO),  $\text{La}_{1-x}\text{Sr}_x\text{MnO}_3$  (LSMO), Electrical Properties

## I. INTRODUCTION

Doped perovskite manganites, exhibiting colossal magneto resistance (CMR) effect have attracted considerable attention not only for fundamental research, but also for potential applications [1, 2]. The magnetic property of ultrafine granular systems is an interesting subject of research for both theoreticians and experimentalists. Considerable difference in magnetization has been observed by varying particle size and have attributed to the presence of nonmagnetic or magnetically dead surface layer [3] or disordered spin orientation in the surface. The nature of interplay between the crystal structure, magnetic and transport properties of manganites is still a matter of discussion in spite of numerous investigations. The size and shape of particle, particle size distribution, and finite size effect and dipolar or exchange interaction between the particle strongly influence the properties of manganites [3,4]. The underlying physical mechanism is that interactions, one ferromagnetic (FM) and the other antiferromagnetic (AFM), shows variety of physical properties in magnetic (FM or AFM), charge (metal, insulator, or charge ordering), and orbital / lattice degrees of freedom [5]. The phenomenon of metal-insulator transition and electronic phase diagram in doped manganese oxides with perovskite structure has not been satisfactorily explained despite extensive efforts [6]. Most of the investigations show that the ferromagnetic Curie temperature and the metal-insulator transition temperatures in such materials are strongly dependent on composition and synthesis condition. A measurable effect, i.e. field induced modulation of resistance, has also been reported in the CMR manganites [7]. This makes the CMR oxides a likely candidate for use as semiconductors in novel field effect transistors with ferroelectric gate. These devices can be interrogated by reading the resistance (or conductance) of the

CMR-based channel. Among all the compositions of  $\text{La}_{1-x}\text{Sr}_x\text{MnO}_3$ , the  $\text{La}_{0.7}\text{Sr}_{0.3}\text{MnO}_3$  shows a variety of structural, electrical and magnetic transitions over a range of temperatures [8]. The physical properties of these materials are usually dependent on their preparation routes [9]. One of the most important aspects is the formation of high quality ceramics and monophonic homogeneous thin films onto the suitable substrates for real applications. For applications a ceramic material consisting of small manganite particles, show a large grain boundary effect at low temperatures could also be interesting. It is therefore important to study the structure and physical properties of the CMR material at nanoscale. The samples with smaller grain sizes possibly show richer electronic and magnetic properties, due to the influence of the structural and magnetic disorders at the grain interfaces. There have been several methods to prepare these manganites by varying micro to nanoparticle size. We choose to prefer sol-gel (SG) technique due to the reason that is, low temperature, quality of precursors, homogeneity of precursors, and particle size can be controlled properly. . In addition, a maximum possibility for quality formation of samples can be achieved in these techniques. The complex impedance spectroscopy (CIS) is a useful technique to analyze the electrical properties of electro ceramics. This technique offers several advantages such as the determination of relaxation frequency anseparation of grain, grain boundary and grain-electrode effects. The complex impedance spectroscopic studies involve measurement of real and imaginary parts of impedance for a wide range of frequency. In recent years, this technique has become a well-accepted fundamental tool for characterizing ionic conductors in terms of ionic conductivity, electrode polarization and activation energy for ion migration. Moreover, this technique has been exploited to probe the solid electrolytes, particularly to distinguish the inter-grain, intra-grain conduction, micro-heterogeneity and electrode material interface. In the present investigation, we have carried out complex impedance formalism and relaxation process of the newly proposed perovskite  $\text{La}_{1-x}\text{Sr}_x\text{MnO}_3$  ( $x=0, 0.15, 0.3, 0.45$ ) ceramic material in the temperature range 30–700<sup>o</sup>C and frequency range 42 Hz to 50 MHz..

## II. EXPERIMENTAL METHOD

Polycrystalline  $\text{La}_{1-x}\text{Sr}_x\text{MnO}_3$  ( $x=0, 0.15, 0.3, 0.45$ ) were prepared using sol-gel method. High purity nitrates were used for the preparation. A stoichiometric mixture lanthanum nitrate and manganese nitrate and Strontium were used as

raw materials. A stoichiometric mixture of nitrates was mixed with citric acid and ethylene glycol and stirred magnetically at 80°C for 3h to obtain a homogenous mixture; the solution was further heated in a pressure vessel at about 130°C for 12 hrs and subsequently kept at 350°C for 3 hrs a muffle furnace and then milled to a fine powder. The dried powder was then calcined in the range of 350°C to 750°C for 6 hrs in order to improve the crystallinity of the powder. The impedance measurement were done on the pellets (the pellets of 13.2 mm diameter and 15.45 mm thickness were made by applying a pressure of 8 tons on the powdered sample) by using an LCR meter. Impedance measurement were carried out in the frequency range 42 Hz-500 MHz and at temperature range 37 to 700°C

### III. RESULT AND DISCUSSION

#### A. STRUCTURAL ANALYSIS

Fig. 1(a) shows the XRD patterns of samples LaMnO<sub>3</sub> and Fig. 1(b) shows XRD pattern of La<sub>0.7</sub>Sr<sub>0.3</sub>MnO<sub>3</sub> calcined at 550°C. The diffraction peaks appearing for the samples ( Fig. 1(a) ) at 2θ values of about 22.9, 32.67, 40.27, 46.89, 52.75, 58.22, 68.63 corresponds to (002), (200), (202), (004), (114), (204), (400) planes of orthorhombic phase of LaMnO<sub>3</sub>. No additional peaks are seen due to addition of Sr in LaMnO<sub>3</sub> because Sr is substituted in the lanthanum site forming a homogeneous mixture shown in Fig.1(b). The particle size was calculated using the Scherrer's formula [10]. The Scherrer formula is given by:

$$D = 0.9 \lambda / \beta \cos \theta \quad \text{----- (1)}$$

where D is the average particle size perpendicular to the reflecting planes, λ is the X-ray wavelength, β is the full width at half maximum (FWHM), and θ is the diffraction angle. The average particle size was found to be about 60 nm. Fig.2 shows the of TEM study LaMnO<sub>3</sub> calcined at 550°C. It can be seen that the particles have nanometer-scale morphology at a relatively low calcination temperature and are well dispersed from each other. The particle size is estimated to be 60nm.

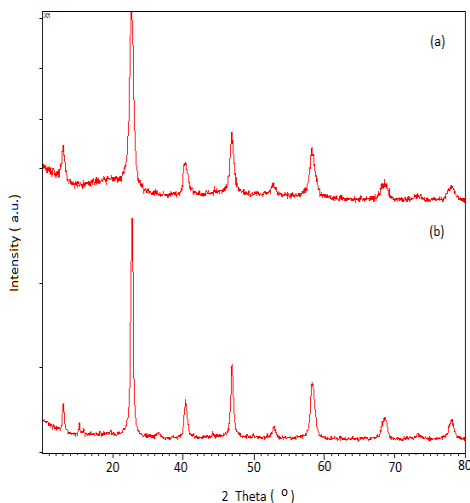


Fig.1 : Fig. 1 XRD patterns of (a) LaMnO<sub>3</sub> and (b) La<sub>0.7</sub>Sr<sub>0.3</sub>MnO<sub>3</sub> calcined at 550°C.

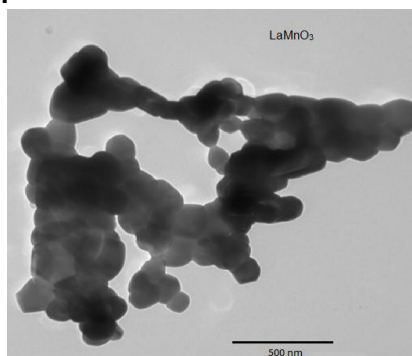


Fig. 2 TEM study LaMnO<sub>3</sub> calcined at 550°C.

Electrical impedance or simply impedance, describes a measure of opposition to alternating current (a.c.) Electrical impedance extends the concept of resistance to a.c. circuits, describing not only the relative amplitudes of the voltage and current, but also the relative phases. When the circuit is driven with direct current (d.c), there is no distinction between impedance and resistance; the latter can be thought of as impedance with zero phase angles. The symbol for impedance is usually *z* and it may be represented by writing its magnitude and phase in the form *z*∠*θ*. However, complex number representation is more powerful for circuit analysis purposes. The term impedance was coined by Oliver Heaviside et al. [11] and Kennelly et al.[12] was the first to represent impedance with complex numbers in 1893. Impedance is defined as the frequency domain ratio of voltage to current. The magnitude of the complex impedance is the ratio of voltage to current amplitude. Complex impedance spectrum (CIS) is a non-destructive and powerful experimental technique for the characterization of micro structural and electrical properties of some electronic materials over a wide range of frequency and temperature [13]. There are many ways by which CIS data may be plotted. In CIS field, where capacitive rather than inductive effects dominate, conventionally one plots Im(*Z*)' ≅ -*Z*' on the y-axis vs. Re(*Z*) ≅ *Z*' on the x-axis to give a complex-plane impedance plot. Such graph have been termed as Nyquist plots. But, it has the disadvantage of not indicating frequency response directly, but may nevertheless be very helpful in identifying conduction processes that all present. The complex impedance equations [14] can be written as

$$Z^* = Z' - j Z'' \quad \text{----- (1)}$$

$$Z' = R / (1 + (\omega RC)^2) \quad \text{----- (2)}$$

$$Z'' = R(\omega RC) / (1 + (\omega RC)^2) \quad \text{---- (3)}$$

where *Z*' and *Z*'' are the real and imaginary components of impedance, ω the angular frequency, *R* and *C* are resistance and capacitance, respectively. *j*<sup>2</sup> = -1, this relation offers wide scope for a graphical analysis of the various parameters under different conditions of temperature or frequency. The systematic procedure for the analysis of a.c. measurements is to plot the results in the complex impedance plane; *Z*' vs *Z*'' . These plots are useful for determining the dominant resistance of the sample. However, these are insensitive to smaller resistances. A separation of the grain and grain

boundary properties has been achieved using an equivalent circuit model in impedance analysis. It is understood that at the peaks of semicircles, the equation [15] can be written as

$$2\pi f_{\max} \tau = 1, \quad \text{----- (4)}$$

here,  $\tau$  is the mean relaxation time

Fig. 3(a-d) shows the variation of  $Z'$  with frequency at different measuring temperatures LMO and LSMO at different temperature. The value of  $Z'$  is higher at lower frequency region and as the frequency increases, the value of  $Z'$  decreases monotonically and attains a constant value at high frequency region at all temperatures. The decrease in the  $Z'$  value at low frequency region in all the compounds indicate that the conductivity of these compounds increases with the increase of frequency due to the increase of hopping of charge carriers between the localized ions. At low frequency, the value of  $Z'$  for these compounds decreases with the increase of temperature and these values merge at high frequency region due to the increase of ac conductivity i.e. existence of negative temperature coefficient of resistance (NTCR) in the compounds. Decrement of  $Z'$  with the increase of temperature and frequency suggests a possible release of space charge and consequently lowering of barrier properties in these materials [16]. For a given temperature, with the increase of Ho concentration in BFO,  $Z'$  increases [see Fig1 (.a-d)] which indicates an enhancement of the bulk resistance of the compounds with the substitution. Provides an insight into the electrical processes having the largest resistance in accordance with equations (2) and (3) [17]. The plots show that  $Z''$  values attain a peak ( $Z''_{\max}$ ) at all measuring temperatures. The magnitude of  $Z''_{\max}$  decreases with temperature indicating decrease in the resistive property of the sample. With the increase of temperature, the peak position of  $Z''$  shifts towards higher frequency side.

Fig. 3 (e-h) shows the frequency dependence of imaginary part of impedance ( $Z''$ ) of LMO and LSMO. It

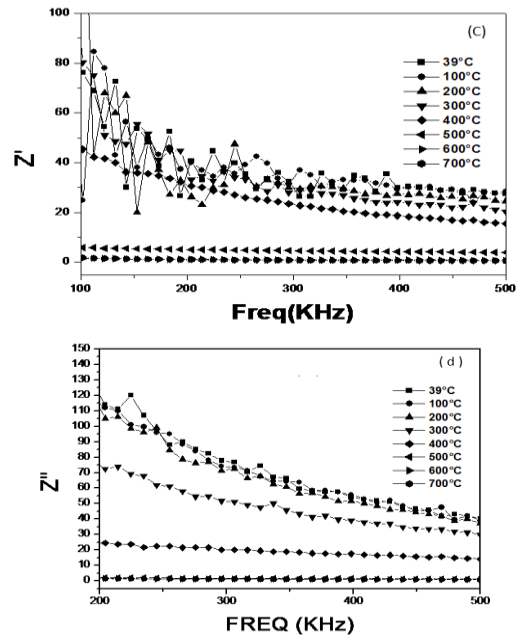
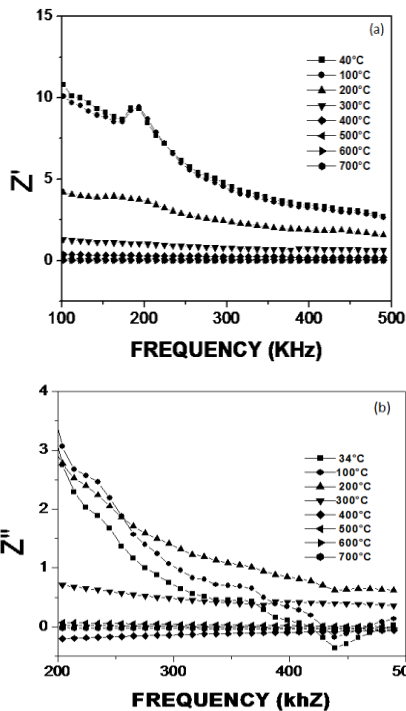
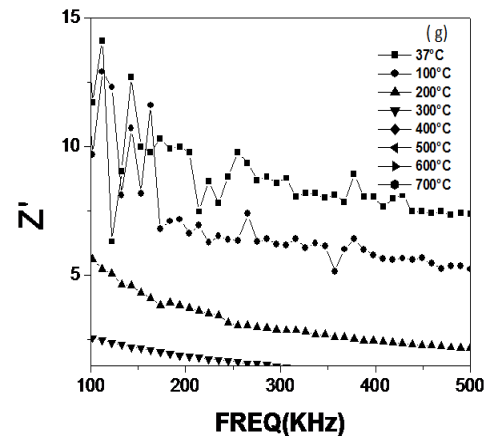
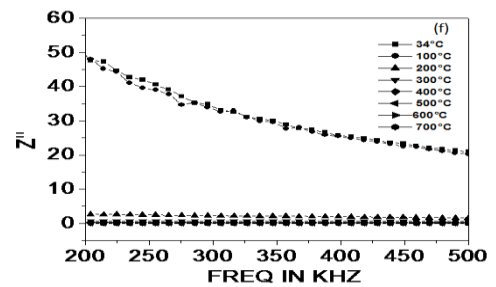
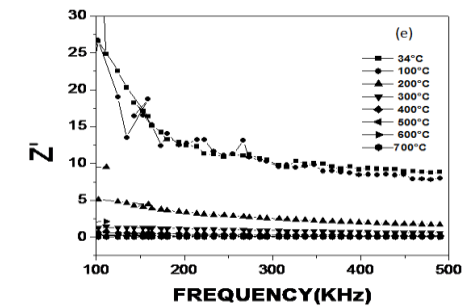


Fig. 3. Frequency dependence of real and imaginary parts of impedance  $Z'$  [(a) LMO, (b), LSMO 0.15, (c), LSMO 0.3 (d) LSMO and  $Z''$



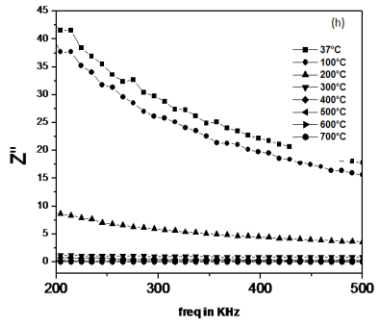


Fig. 3. Frequency dependence of real and imaginary parts of impedance  $Z'$  [LMO-(e), LSMO 0.15 (f), LSMO 0.3 (g) LSMO 0.45 (h)] and  $Z''$

The shift in the peak frequency is because of the presence of electrical relaxations in the material and increase in the rate of hopping of charge carriers. This relaxation is a temperature dependent relaxation. Asymmetric broadening of peaks indicates distribution of spread of relaxation time [18]. The magnitude of  $Z''$  at  $f_{max}$  decreases with the temperature indicating the presence of space charge polarization at low frequency which disappears at high frequency [19]. The magnitude of  $Z''$  at  $f_{max}$  increases with the increase of Sr content. The peak in the  $Z''$  data shifted in the low frequency side with the increase of Sr. This may be attributed to a phenomenon with maximum capacitive effects on Sr substitution. Figure 4 (a-d) shows the  $\log \sigma_{ac} - \log f$  plot of frequency dependence of ac conductivity for LSO and LSMO sample at different temperatures. It is obvious that the conductivity increases with increasing frequency and increasing temperatures shown in Fig. 2 (a-d). At higher temperatures, a plateau is observed in the conductivity plots at lower frequency range where  $\sigma_{ac}$  frequency-independent. The plateau region extends to higher frequencies with the increase of temperature. Notice that at low frequencies, random diffusion of charge carriers via hopping gives rise to a frequency-independent conductivity. At higher frequencies,  $\sigma_{ac}$  exhibit dispersion, increasing in a power law fashion and eventually becoming almost linear. The real part of conductivity  $\sigma$  in such a situation can be given by Jonscher power law [20]

$$\sigma = \sigma_{dc} \left[ 1 + \left( \frac{\omega}{\omega_H} \right)^n \right]^{-1} \quad (7)$$

Where  $\sigma_{dc}$  is the dc conductivity,  $\omega_H$  is the hopping frequency of charge carriers and n is the dimensionless frequency exponent.

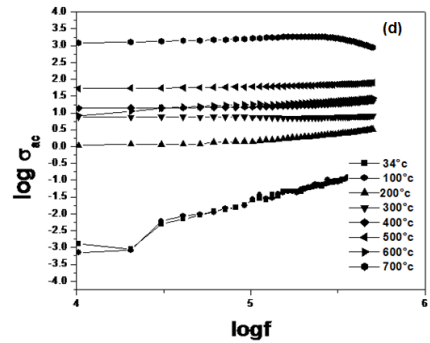
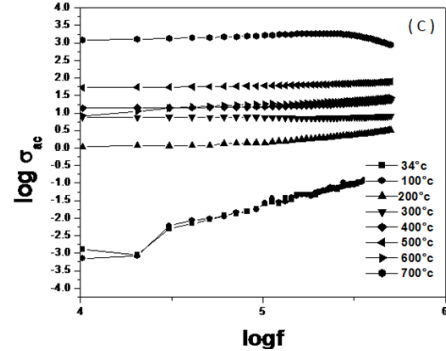
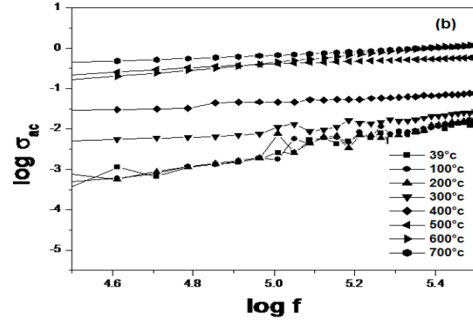
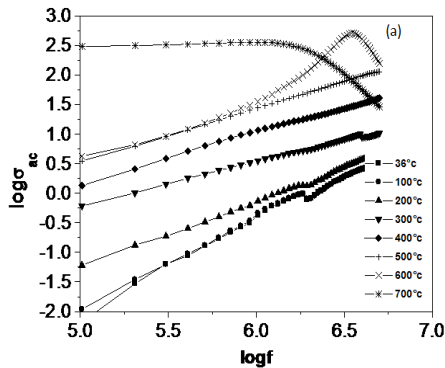
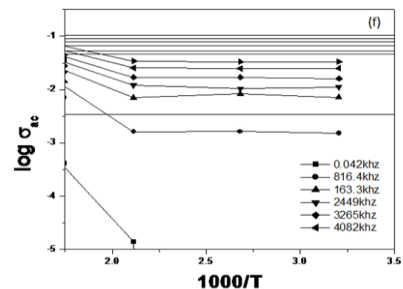
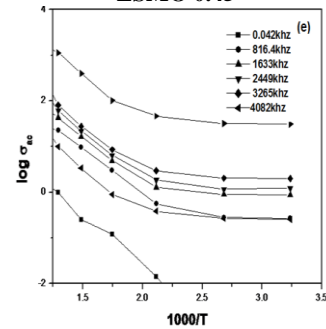
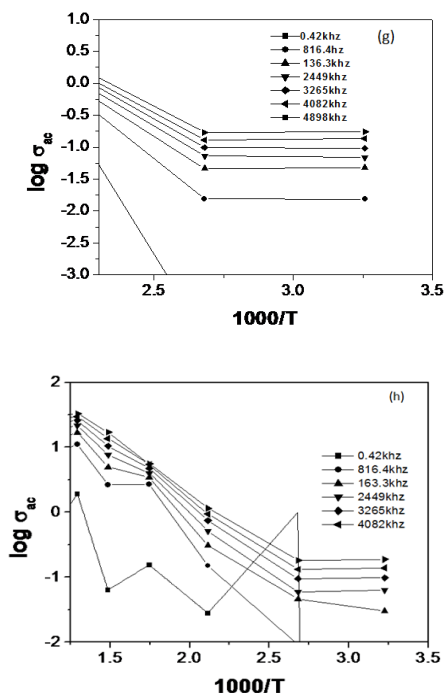


Fig 4 (a-d) :  $\log \sigma_{ac} - \log f$  plot of frequency dependence of ac conductivity for LSO and LSMO sample at different temperatures of (a) LMO,(b) LSMO 0.15, (c) LSMO 0.3 (d) LSMO 0.45





**Fig. 4. Arrhenius plot of ac conductivity of LMO and LSMO at various frequencies (e) LMO (f) LSMO 0.15, (g) LSMO 0.3 (h) LSMO 0.45 at various frequencies**

Figure 4(e-h) shows the Arrhenius plot of ac conductivity of LMO and LSMO at various frequencies. It is interesting to note that ac conductivity activation energy decreases with increasing frequency and different temperature regions in the conduction process.

#### IV. CONCLUSION

A series of polycrystalline  $\text{La}_{1-x}\text{Sr}_x\text{MnO}_3$  ( $x=0,0.15, 0.3,0.45$ ) samples have been synthesized by sol-gel method. X-ray diffraction analysis revealed the nanocrystalline nature in the prepared sample. The XRD pattern of  $\text{La}_{0.7}\text{Sr}_{0.3}\text{MnO}_3$  shows perovskite-type with orthorhombic structure. The electrical conductivity studies showed the NTCR character of LMO and LSMO. The ac conductivity found to obey universal power law and showed the negative temperature coefficient of resistance character. The frequency variation of ac conductivity at different temperatures indicates that the conduction process is thermally activated.

#### REFERENCES

[1] E. Dagotto, *Science* **309**, 257 (2005).  
 [2] Q.A. Pankhurst, J. Connolly, S.K. Jones, J. Dobson, *J. Phys. D: Appl. Phys.* **36**, R167 (2003).  
 [3] M.B. Salamon, M. Jaime, *Rev. Mod. Phys.* **73**, 583 (2001).  
 [4] S. Roy, I. Dubenko, D.D. Edorh, N. Ali, *J. Appl. Phys.* **96**, 1202 (2004).  
 [5] M. Suzuki, S.I. Fullem, I.S. Suzuki, L. Wang, C. Zhong, *Phys. Rev. B* **79**, 024418 (2009).  
 [6] P.E. Jonsson, *Adv. Chem. Phys.* **128**, 191 (2004).  
 [7] Y. Motome, N. Furukawa, *Phys. Rev. B* **71**, 014446 (2005).

[8] P. Dey, T.K. Nath, U. Kumar, P.K. Mukhopadhyay, *J. Appl. Phys.* **98**, 014306 (2005).  
 [9] M. Paraskevopoulos, F. Mayr, C. Hartinger, A. Pimenov, J. Hemberger, P. Lunkenheimer, A. Loidl, A.A. Mukhin, V.Y. Ivanov, A.M. Balbashov, *J. Magn. Mater.* **211,118(2000)**  
 [10] T.P. Sharma, D. Patidar, N.S. Saxena, K. Sharma, *Ind. J. Pure & Appl. Phys.* **44**, 125 (2005).  
 [11] Oliver Heaviside 1886 *The Electrician*, p. 212, 23rd July 1886,  
 [12] Kennelly Arthur 1893 *Impedance (IEEE)*  
 [13] Ivanova V V, Kapyshev A G, Venevtsev Yu N and Zhadanov G S *Izv. ANSSSR, Ser. Fiz.* **26** 354(1962)  
 [14] Chaisan W, Yimnirun R, Ananta S and Cann D P *Mater. Lett.* **59** 3732(2005)  
 [15] Adamczyk M, Ujma Z, Szymczak L, Soszynski A and Koperski J. *Mater. Sci. Eng.* **B136** (2007)pp170  
 [16] A. Kumar, B. P. Singh, R. N. P. Choudhary and A. K. Thakur, *Mater. Chem. Phys.* **99**, 150 (2006)  
 [17] Tiwari Balgovind and Chuadhari R.N. *J. Phys. ( Chem Solid)* **60**, 2852 (2008)  
 [18] C.K. Suman, K. Prasad, R.N.P. Choudhary, *Adv. Appl. Ceram.* **104**, 204(2005).  
 [19] S. Sen, S.K. Mishra, S.K. Das, A. Tarafdar, *J. Alloys Compd.* **453** (2008) 395.  
 [20] Jonscher AK (1983) *Dielectric relaxation in solids*. Chelsea Dielectric Press, London